ΔS° = entropy of vaporization at normal boiling point, cal./° C. mole
ΔS_p° = ΔS° for the corresponding normal paraffin having $n = n_0^*$
T = temperature, ° C.
T_b = boiling point, ° C.
T_b° = normal boiling point, ° C.
t = constant in Equation 15
Λ = heat of vaporization, kcal./mole
Λ° = heat of vaporization at normal boiling point, kcal./mole

LITERATURE CITED

(1) Am. Petrol. Inst., Research Project 44, Data Sheets, Chemical Thermodynamic Properties Center, A. and M. College of Texas, College Station, Texas.
(2) Cox, E.R., *Ind. Eng. Chem.* **15**, 592 (1923).
(3) Dreisbach, R.R., "Physical Properties of Chemical Compounds-III," *Advanc. Chem. Ser.*, No. **29**, Am. Chem. Soc., Washington, D. C., 1961.
(4) Duhling, U., *Ann. Physik* **11**, 163 (1880).
(5) Lippincott, S.M., Lyman, M.M., *Ind. Eng. Chem.* **38**, 320 (1946).
(6) Mfg. Chemists' Assoc., Research Project, Data Sheets, Chemical Thermodynamic Properties Center, A. and M. College of Texas, College Station, Texas.
(7) Nakanishi, K., *J. Fac. Eng. Shinshu Univ.*, No. **11**, 37 (1961).
(8) Nakanishi, K., *Ibid.*, to be published.
(9) Nakanishi, K., Kurata, M., Tamura, M., J. Chem. Eng. Data **5**, 210 (1960).
(10) Othmer, D.F., *Ind. Eng. Chem.* **32**, 841 (1940).
(11) Reckhard, H., *Chem. Ztg.* **84**, 33 (1960).
(12) Reid, R.C., Sherwood, T.K., "The Properties of Gases and Liquids: Their Estimation and Correlation," McGraw-Hill, New York, 1958.
(13) Stull, D.R., *Ind. Eng. Chem.* **39**, 517 (1947).
(14) Tamura, M., Kurata, M., Nakanishi, K., Nagata, I., *Bull. Chem. Soc. Japan* **34**, 684 (1961).
(15) Timmermans, J., "Physico-chemical Constants of Pure Organic Compounds," Elsevier, 1950.

Received for review May 22, 1962. Accepted January 23, 1963.

Cryoscopic Investigations and Phase Equilibria

H. C. KO, T. HU, J. G. SPENCER, C. Y. HUANG and L. G. HEPLER
Contribution from Departments of Chemistry, University of Virginia, Charlottesville, Va., and Carnegie Institute of Technology, Pittsburgh, Pa.

Partial phase diagrams have been determined for the $NaNO_3$–$NaCl$, $NaNO_3$–$Ba(NO_3)_2$, $NaNO_3$–Na_2MoO_4, and KNO_3–KCl systems by means of cooling curves and direct solubility determinations, and eutectic temperatures and compositions are reported. Freezing point depressions for dilute solutions of various salts in $NaNO_3$ and KNO_3 have been measured differentially and used to calculate heats of fusion.

WE HAVE determined partial phase diagrams for the $NaNO_3$-$NaCl$, $NaNO_3$-$Ba(NO_3)_2$, $NaNO_3$-Na_2MoO_4, and KNO_3-KCl systems and have made precise measurements of freezing point depressions in $NaNO_3$ and KNO_3 from which we have calculated heats of fusion. Phase diagrams have been deduced from cooling curves and direct solubility determinations. Freezing point depressions have been measured more precisely than is customary for investigations of dilute molten salt solutions.

EXPERIMENTAL

Chemicals. All chemicals were of C.P. grade and were dried by heating before they were used. $BaCl_2$ was obtained by dehydration of $BaCl_2 \cdot 2H_2O$ at about 120° C. until weight was constant.

Apparatus and Procedure. A cylindrical aluminum block surrounded by Kaylo insulation in a chemical drum has been used as a furnace. Holes were drilled in the aluminum block to accommodate two borosilicate glass sample tubes and one junction of a thermocouple. Other holes were drilled in the block and slots were milled around the circumference of the block to accommodate Nichrome heaters.

For cooling curve experiments one of the test tubes in the block was charged with a 40-gram sample of the desired composition. The sample and block were heated by the block heaters to 25° C. above the liquidus temperature and maintained at this temperature for several minutes. Then the block and sample were allowed to cool at a rate of about 0.8° per minute.

The sample tube contained a 5-mm. borosilicate glass tube to protect two Chromel-Alumel thermocouple junctions. One of these junctions was connected to a reference junction at 0° C. and gave the temperature of the sample. The other junction in the sample was connected to a reference junction in a hole in the block, as suggested by Beusman (*1*). A helical glass stirrer in the test tube was moved up and down over a 2-inch stroke at a rate of 57 strokes per minute by a motor. An aluminum cap with holes for the thermocouple tube and stirrer fitted over the top of the sample tube.

One thermocouple was calibrated at the boiling point of water and the freezing points of lead, tin, and zinc with the recorder later used for recording cooling curves.

Because of difficulty in detecting the change in slope of the cooling curve that corresponds to the liquidus temperature, we also recorded the output of the thermocouple with its reference junction in the block. When the liquidus temperature was reached, the output of this thermocouple increased sharply, and clearly indicated the time corresponding to the liquidus temperature on the cooling curve. Liquidus temperatures were determined in this way to ±0.5°. Eutectic temperatures were obtained directly from the cooling curves to ±0.5°.

When experiments like those described above are carried out separately on solutions and on the pure major component of the solutions, freezing point depressions are calculated as the difference in liquidus temperatures. We have used another procedure that is better for such investigations of dilute solutions. One tube in our apparatus was loaded with the pure major component and the other with a mixture of the desired composition. After both samples were completely melted and in equilibrium with the block, the block was allowed to cool at a rate of about

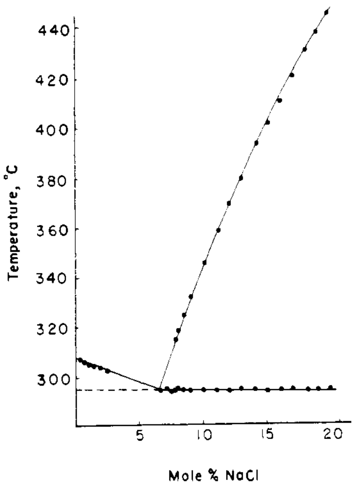

Figure 1. Partial phase diagram for $NaNO_3$–NaCl system

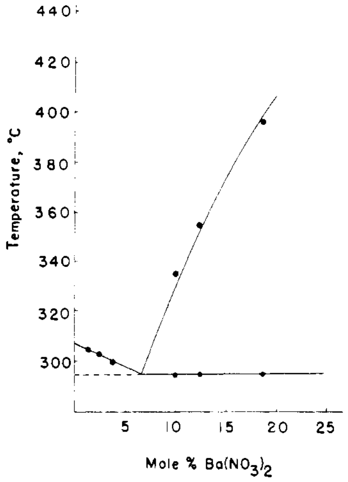

Figure 2. Partial phase diagram for $NaNO_3$–$Ba(NO_3)_2$ system

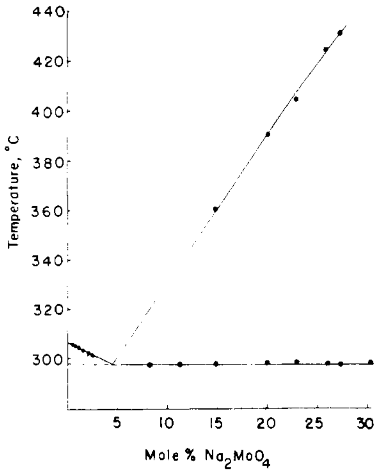

Figure 3. Partial phase diagram for $NaNO_3$–Na_2MoO_4 system

0.8 degree per minute. The pure substance first began to freeze and its temperature remained constant until freezing was complete. The major component in the second tube later began to freeze out before freezing in the first tube was complete. The output of a two-junction Chromel-Alumel thermel with one pair of junctions in each tube gave directly at this time the freezing point depression.

Experiments with different amounts of pure salt in the reference tube were carried out to show that our results did not depend on the fraction of solvent frozen in the reference tube.

The two-junction thermel was calibrated by placing one pair of junctions in a tube containing solid and liquid sodium nitrate in equilibrium and the other pair in a tube containing solid and liquid sodium nitrite or solid and liquid lead in equilibrium. Output of this thermel was found to be 81.8 μv. per degree.

Freezing point depressions were determined to about ±0.03° with a recorder and about ±0.01° with a Leeds and Northrup K3 potentiometer.

Solubility determinations were made in a $NaNO_3$-KNO_3 constant temperature bath controlled to ±0.5°. Samples were placed in test tubes in the bath and allowed to remain there with occasional stirring until equilibrium was attained, as proved by analysis of samples removed at different times. Then samples were removed for analysis with a small preheated breaker on the end of a thin glass rod.

RESULTS AND CALCULATIONS

Partial phase diagrams for the systems $NaNO_3$-NaCl, $NaNO_3$-$Ba(NO_3)_2$ and $NaNO_3$-Na_2MoO_4 are shown in Figures 1, 2, and 3. Eutectic data are summarized in Table I.

The phase diagram for the $NaNO_3$-Na_2MoO_4 system is based on results of cooling curve experiments for compositions richer in Na_2MoO_4 than the eutectic composition and on freezing point lowering measurements for compositions richer in $NaNO_3$ than the eutectic composition. The phase diagram for the $NaNO_3$-$Ba(NO_3)_2$ system is based on cooling curve experiments for compositions richer in $Ba(NO_3)_2$ than the eutectic composition and on solubility determinations over the range up to 25 mole % $Ba(NO_3)_2$. The phase diagram for the $NaNO_3$-NaCl system is based on cooling curve data for the range of compositions richer in NaCl than the eutectic composition, on freezing point lowering data for solutions richer in $NaNO_3$ than the eutectic composition, and on solubility data over the range of compositions up to 20 mole % NaCl. Agreement is good where data from different kinds of measurements overlap.

Table I. Eutectic Data on $NaNO_3$–NaCl, $NaNO_3$–$Ba(NO_3)_2$, and $NaNO_3$–Na_2MoO_4 Systems

System	Eutectic Composition, Mole %	Eutectic Temp., ° C.
$NaNO_3$-NaCl	6.6 NaCl	294.4 ± 0.5
$NaNO_3$-$Ba(NO_3)_2$	6.7 $Ba(NO_3)_2$	295.2 ± 0.8
$NaNO_3$-Na_2MoO_4	4.5 Na_2MoO_4	298.3 ± 0.3

The partial phase diagram for the KNO_3-KCl system up to 25 mole % KCl, based on solubility determinations, is shown in Figure 4. The eutectic temperature is 320.5° C. and the eutectic composition is 5.85 mole % KCl. The peritectic temperature is 361° C. with corresponding composition of 16.0 mole % KCl.

Thermodynamic treatment (5) of dilute solutions leads to the equation:

$$\Delta T = \frac{RT^2 M_1 im}{1000\,\Delta H_1} = K_f\, im \qquad (1)$$

M_1 is the molecular weight of the major component, m is the molality, ΔH_1 is the heat of fusion of the major component, and i is the number of moles of foreign ions per mole of minor component.

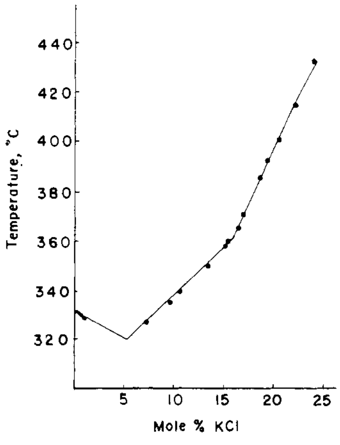

Figure 4. Partial phase diagram for KNO_3–KCl system

Freezing point lowering measurements were made on dilute solutions of NaCl, Na_2MoO_4, Na_2WO_4, KCl, and $BaCl_2$ in $NaNO_3$. Graphs of our experimental ΔT values against the corresponding molalities were straight lines whose slopes yielded the values of iK_f given in Table II with derived values for the heat of fusion of $NaNO_3$.

The "best" value for the heat of fusion of $NaNO_3$ calculated from our results is 3600 ± 100 cal./mole.

Freezing point depression measurements were also carried out on dilute solutions of KCl in KNO_3. The slope of the straight line in a graph of ΔT against m led to K_f = 23.9° C. per mole of foreign ions and ΔH_1 = 3080 cal./mole for the heat of fusion of KNO_3.

DISCUSSION

Equation 1 is valid only for dilute solutions from which the pure major component is frozen out as the temperature is lowered. We found no evidence for solid solution formation in any of the systems discussed in this paper.

Perman (*9*) made a few freezing point measurements in the $NaNO_3$-rich region of the $NaNO_3$-NaCl system. Nyankovskaya (*7*) studied the NaCl-$NaNO_3$-KCl-KNO_3 system over wide ranges of composition and temperatures. Our results are in good agreement with results of these earlier workers, although their data for dilute solutions are not precise enough to permit accurate evaluation of heats of fusion. Laybourn, Madgin, and Freeman (*6*) studied the $NaNO_3$–$Ba(NO_3)_2$ system and reported the eutectic temperature and composition to be 284° C. and 6.37 mole % $Ba(NO_3)_2$, in poor agreement with our results. Lifshits (*8*) reported that the system of KNO_3-KCl has an eutectic point at 320° C. (6 mole % KCl) and that the eutectic is composed of KNO_3 and $KNO_3 \cdot KCl$. He also reported a transition point at 360° C. (17.4 mole % KCl) with the solution composed of KCl and $KNO_3 \cdot KCl$. These conclusions are in agreement with our results.

The cryoscopic data of Van Artsdalen (*10*) lead to 3780 cal./mole for the heat of fusion of $NaNO_3$. Kelley (*4*) has recently reviewed the literature and listed the heat of fusion of $NaNO_3$ as 3490 cal./mole and in earlier reviews (*2*, *3*) listed values from 3160 to 3800 cal./mole. Our value is 3600 cal./mole.

Table II. Freezing Point Constant and Heat of Fusion of $NaNO_3$

Minor Component	iK_f	ΔH_1, Cal./Mole
NaCl	15.7	3610 ± 100
Na_2MoO_4	16.0	3550 ± 100
Na_2WO_4	15.4	3700 ± 200
KCl	31.6	3600 ± 100
$BaCl_2$	50.2	3400 ± 250

In his recent review (*4*) Kelley has taken the heat of fusion of KNO_3 to 2800 cal./mole and earlier (*2*) listed values ranging from 2910 to 3040 cal./mole. Our value is 3080 cal./mole.

ACKNOWLEDGMENT

We thank Mr. Frank J. Millero for his help with some of the experiments and calculations.

LITERATURE CITED

(1) Beusman, C., Oak Ridge National Laboratory Report, ORNL-**2323**, 1957 (unclassified).
(2) Kelley, K.K., U. S. Bur. Mines *Bull.* **393**, 1936.
(3) *Ibid.*, **476**, 1949.
(4) *Ibid.*, **584**, 1960.
(5) Klotz, I.M., "Chemical Thermodynamics," Prentice-Hall, Englewood Cliffs, N. J., 1956.
(6) Laybourn, K., Madgin, W.M., Freeman, D., *J. Chem. Soc.*, **39** (1934).
(7) Levin, E.M., McMurdie, H.F., "Phase Diagrams for Ceramists," Figure 1421, The American Society, Inc., Columbus, Ohio, 1959.
(8) Lifshits, G.M., *Zh. Obshch. Khim.*, **25**, 2414 (1955); *Chem. Abstr.* **50**, 9127g (1956).
(9) Perman, E.P., *J. Chem. Soc.*, 2473 (1922).
(10) Van Artsdalen, E.R., *J. Phys. Chem.*, **60**, 172 (1956).

RECEIVED for review May 4, 1962. Accepted December 28, 1962. We are grateful to the Atomic Energy Commission for support of the first part of this work at the University of Virginia and the remainder at the Carnegie Institute of Technology.

Effect of Catalysts on Burning Rate of Ammonium Nitrate

A. GREENVILLE WHITTAKER[1] and DAVID C. BARHAM
Sandia Corporation, Albuquerque, N.M.

EARLY IN OUR efforts to determine the temperature profile and surface temperature of burning ammonium nitrate, a combustion catalyst was needed to get sustained combustion in a convenient pressure range. It introduced much "noise" in the temperature profile measurements; therefore an exploratory study was made on the effect of catalysts on the combustion of ammonium nitrate to determine the minimum catalyst concentration that would yield a system suitable for temperature profile measurements. This turned out to be 2.5% chromic oxide. The "noise" due to the catalyst particles seemed to be independent of particle size as long as they were less than 70 mesh (U. S. standard sieve). In the course of this brief study, some observations were made that may be of interest to investigators working in other fields.

EXPERIMENTAL

Reagent grade ammonium nitrate was used without further purification. It was ground to pass through a 200-mesh U. S. standard sieve and dried in a vacuum desiccator over Drierite. The ammonium dichromate was prepared similarly. Chromic oxide catalyst was obtained by thermal decomposition of ammonium dichromate. This chromic oxide was screened and only the fraction passing

---

[1] Present address, Aerospace Corp., Laboratories Division, 2400 E. El Segundo Blvd., El Segundo, Calif.